Journal of Controlled Release 243 (2016) 243–249

Contents lists available at ScienceDirect

Journal of Controlled Release

journal homepage: www.elsevier.com/locate/jconrel

Liposomal prednisolone inhibits tumor growth in a spontaneous mouse mammary carcinoma model

Anil K. Deshantri [a,1], Sander A.A. Kooijmans [a,c,1], Sylvia A. Kuijpers [b], Maria Coimbra [b], Astrid Hoeppener [b], Gert Storm [b], Marcel H.A.M. Fens [a], Raymond M. Schiffelers [a,b,*]

[a] Department of Clinical Chemistry and Haematology, University Medical Center Utrecht, Utrecht, The Netherlands
[b] Department of Pharmaceutics, Utrecht Institute for Pharmaceutical Sciences, Utrecht University, Utrecht, The Netherlands
[c] Department of Medical Sciences, University of Torino, Torino, Italy

ARTICLE INFO

Article history:
Received 8 September 2016
Accepted 13 October 2016
Available online 20 October 2016

Keywords:
Liposomes
Prednisolone
Spontaneous breast cancer
miRNAs

ABSTRACT

Cancers are abundantly infiltrated by inflammatory cells that are modulated by tumor cells to secrete mediators fostering tumor cell survival and proliferation. Therefore, agents that interfere with inflammatory signaling molecules or specific immune cell populations have been investigated as anticancer drugs.

Corticosteroids are highly potent anti-inflammatory drugs, whose activity is intensified when targeted by nanocarrier systems. Liposome-targeted corticosteroids have been shown to inhibit tumor growth in different syngeneic murine tumor models as well as human xenograft mouse models, which is attributed to a switch in the tumor microenvironment from a pro-inflammatory to an anti-inflammatory state. Despite the recognized value of implantation tumor models in preclinical research, the "acute" inflammation induced by inoculation of tumor cells together with the exponential tumor growth in a relatively short period of time does not resemble slow progressive human disease that develops in situ. Therefore, in this study, the antitumor effect of liposomal corticosteroids was investigated in a clinically more relevant setting of transgenic mice developing spontaneous breast carcinomas.

Here we show that liposomal prednisolone phosphate inhibits the growth of spontaneous breast carcinoma. Interestingly, the liposomal prednisolone was significantly more active than free drug. At 72 h after injection of the liposomal formulation, 3 μg prednisolone per gram of tumor tissue was recovered whereas no drug could be recovered after injection of the free agent. This indicates that, despite etiological and morphological differences between implanted and spontaneous tumor models, EPR-mediated accumulation of drug occurs to similar extent in this spontaneous mammary carcinoma model as in the syngeneic tumor models.

Finally, we analyzed miRNA profiles in the MMTV/*neu* model and showed that the top 10 of miRNAs in the MMTV/*neu* tumor consisted of miRNAs with a known involvement in breast carcinoma proliferation and metastasis. The only exception was the appearance of miR-146b, a known inflammation-regulating miRNA species, after liposomal prednisolone treatment.

1. Introduction

Tumors are complex assemblies of multiple cell types in a net favorable environment for their survival, growth, invasion and dissemination. Cancer growth, invasion and metastasis appear largely dependent on the ability of the mutated malignant cells to hijack and exploit physiological processes of the host. A dysfunctional inflammatory response is one of the hallmarks of cancer [1–3]. Several malignancies arise at sites of chronic infection (e.g. Hepatitis B virus infection, *Helicobacter pylori* infection) and inflammation (autoimmune diseases, such as inflammatory bowel disease) [4]. But also after tumor initiation, the microenvironment of a developing tumor often harbors a large infiltrate of innate and adaptive immune cells and associated inflammatory mediators [5]. Whereas full activation of innate and especially adaptive immune cells may translate in eradication of the mutant cells, the chronic activation of inflammatory cells within the tumor microenvironment is known to support tumor proliferation, survival and migration. Activated inflammatory cells produce signaling mediators (cytokines, chemokines, growth factors), in general to ensure protection against injury and promote tissue homeostasis. In cancer, these processes seem to be co-opted by the tumor cells to foster cell survival and proliferation and reach an immune privileged status. This offers the

* Corresponding author at: Hematology Room G 03.647 UMC Utrecht, Heidelberglaan 100, 3584 CX Utrecht, The Netherlands. PO Box 85500, 3508 GA Utrecht, The Netherlands.
E-mail addresses: R.M.Schiffelers@uu.nl, R.Schiffelers@umcutrecht.nl (R.M. Schiffelers).
[1] These authors contributed equally to this work.

http://dx.doi.org/10.1016/j.jconrel.2016.10.016
0168-3659/

possibility for therapeutic strategies that are aimed at interfering with these signaling molecules and specific immune cell-subtypes to modulate -and ultimately shift- the inflammatory microenvironment towards an anti-tumor phenotype [6,7].

One of the promising classes of compounds to achieve such a shift are steroidal anti-inflammatory drugs [8]. They possess strong anti-inflammatory and immunomodulatory activities that translate in anti-tumor effects in vitro and in vivo. Various genomic and non-genomic mechanisms of action could mediate this therapeutic effect. Genomic effects already seem to take place at low concentrations of corticosteroids, while non-genomic mechanisms require higher concentrations. A combination of both types of effects appears to be necessary as antitumor activities are achieved only at very high doses. These concomitantly can lead to the occurrence of severe adverse effects inherent to the strong systemic immunosuppression, which can even lead to death due to opportunistic infections [9].

The therapeutic index of corticosteroids and their anti-inflammatory effects can be substantially increased by incorporation of corticosteroids in nanocarrier-platforms such as polymeric micelles and liposomes [10–13]. The leaky architecture of the tumor vasculature tissues allows the passive delivery of long-circulating nanomedicines to the tumor tissue by the "enhanced permeability and retention (EPR) effect" but also macrophage-rich organs like liver, spleen and bone marrow are targeted, which could also be involved in the therapeutic effect [14]. The distribution of the drug to other sites is limited, reducing the occurrence of certain side effects.

The antitumor activity of liposomal corticosteroids has been studied in different subcutaneous murine tumor models, particularly in B16F10 melanoma and C26 colon carcinoma [15]. In both experimental models, a single intravenous administration of prednisolone encapsulated in long-circulating liposomes (LCL-PLP) inhibited tumor growth in a dose-dependent manner.

By definition, animal models are an approximation of human disease. However, spontaneous tumor models are likely to be closer to the clinical situation than the transplantation models that we have used thus far [16,17]. The acute injection of a mass of ex vivo cultured tumor cells may contain a different inflammatory milieu than spontaneous tumors. A frequent concern in developing new anti-cancer drugs is the difficulty to predict drug activity in human disease when employing murine tumor models. Thus, more advanced, genetically engineered mouse tumor models may better predict the ultimate clinical activity of drug molecules, since such models display orthotopic primary tumors in an immune competent setting [18].

In this study, we investigated the accumulation in the tumor and antitumor effects of LCL-PLP in transgenic mice that carry the unactivated *neu* (Erbb2) oncogene under the control of the mouse mammary tumor virus (MMTV). This mouse model is characterized by the spontaneous development and slow growth of breast cancer over a period of months [19].

2. Materials and methods

2.1. Liposome preparation

Liposomes were prepared as described previously [12]. In brief, appropriate amounts of dipalmitoylphosphatidylcholine (Lipoid GmbH, Ludwigshafen am Rhein, Germany), cholesterol (Sigma-Aldrich, Germany), and poly (ethylene glycol) 2000-distearoylphosphatidylethanolamine (Lipoid GmbH), in a molar ratio of 1.85:1.0:0.15 respectively, were dissolved in ethanol in a round-bottom flask. A lipid film was prepared under reduced pressure on a rotary evaporator and dried under a stream of nitrogen until complete dryness. Liposomes were prepared by rehydration of the lipid film with a solution of 100 mg/ml prednisolone disodium phosphate (BUFA, The Netherlands). Liposome size was reduced by multiple extrusion steps (Lipex high pressure extruder, Northern Lipids) using polycarbonate membranes (Whatman, Nuclepore) with a final pore size of 50 nm. Mean particle size of the liposomes was determined by dynamic light scattering with a Malvern ALV CGS-3 system and found to be 0.1 μm in a monodisperse system. Total lipid content of the liposomal dispersion was determined with a phosphate assay on the organic phase after extraction of liposomal preparations with chloroform and according to Rouser et al. [20]. Liposomal dispersion was transferred to a Slide-A-Lyzer cassette (Thermo Scientific, Waltham, MA, USA) with a molecular weight cut-off of 10 kD in order to remove unencapsulated drug by dialysis at 4 °C with repeated changes of buffer. The aqueous phase after chloroform extraction was used for quantification of prednisolone phosphate by Ultra Performance Liquid Chromatography (UPLC, Waters Acquity UPLC- TUV system, Waters Corporation, Milford, MA, USA). Measurements were performed using an Acquity BEH C18 1.7 μm column (2.1 × 50 mm, Waters) and the mobile phase consisted of acetonitrile (Biosolve, Valkenswaard, The Netherlands) and water (25:75 (v/v)), brought to pH 2 with perchloric acid (Mallinckrodt Chemicals, Chesterfield, UK). Detection was performed by a diode array detector set at a wavelength of 254 nm. The liposomal preparation contained approximately 5 mg of prednisolone/ml and 60 μmol lipid/ml. The liposome suspension was stored at 4 °C.

2.2. Inhibition of cell proliferation

MCF-7 cells (ATCC HTB-22) and MDA-MB-231 (ATCC HTB-26) human mammary carcinoma cells were incubated with PLP, LCL-PLP or liposomes as control (C). Cells were cultured in DMEM/F12 medium (Life Technologies Europe B.V., Bleiswijk, The Netherlands) containing 1.2 g/L sodium bicarbonate, 3.6 g/L HEPES, 3.2 g/L D-glucose, 2.5 mM L-glutamine, and supplemented with 10% FBS. 10^3 cells/well were plated in a 96-well plate for 24 h. Subsequently, liposomal PLP and free PLP or vehicle were added in the respective wells. The anti-proliferative effect was determined over 48 h, by ELISA BrdU-colorimetric immunoassay (Roche Applied Science, Penzberg, Germany) according to the manufacturer's instructions. This technique is based on the incorporation of the pyridine analogue bromodeoxyuridine (BrdU) instead of thymidine into the DNA of proliferating cells. To detect BrdU incorporated in newly synthesized cellular DNA, a monoclonal antibody conjugated with peroxidase was added. After 90 min of incubation, cell lysates were washed three times with PBS. The immune complexes were detected by adding the substrate of peroxidase (tetramethyl-benzidine). The reaction product was quantified by measuring the absorbance at 450 nm with a reference wavelength of 655 nm.

2.3. In vivo studies

Transgenic female mice FVB/N-Tg (MMTV/*neu*) 202Mul/J (12–13 weeks age) were purchased from Jackson Laboratory (USA). Mice were kept in standard housing on a 12 h light/dark cycle with standard rodent chow and water available ad libitum. Experiments were performed in accordance to the national regulations and were approved by the local animal experiments ethical committee. Transgenic mice developed mammary tumors spontaneously within 3 to 7 months upon arrival, as described earlier [19]. Tumors were measured daily with a digital calliper and the tumor volume was calculated according to the formula: $V = 1/6\pi a^2 b$, where a is the smallest and b the largest superficial diameter. In a small number of mice, tumor growth was extremely fast going from palpable to over 200 mm^3 within 1 week. These mice were excluded as they deviate from the tumor growth curve that has been described for this model. Mouse weight was recorded in order to monitor weight loss as a result of toxic side effects. To evaluate the therapeutic effects of corticosteroids in a spontaneous tumor model, transgenic mice received 20 mg/kg of free or liposomal prednisolone phosphate or an equivalent volume of vehicle, intravenously via the tail vein when mammary tumors reached a size of 200 mm^3. The dose

was based on therapeutic activity of liposomal prednisolone in transplantation models [15]. Treatments were given to mice once weekly until endpoint was reached, i.e., tumor volume of 1500 mm^3 or therapy was given for a maximum of 10 weeks. At this time, mice were sacrificed by asphyxiation with CO_2, tumors were harvested and snap frozen in liquid nitrogen.

2.4. Drug accumulation in tumor tissue

Prednisolone phosphate concentrations in tumor tissue were analyzed as described previously [15] with slight modifications regarding homogenization of tissues. When mammary tumors reached 200 mm^3, mice received a single intravenous administration of 20 mg/kg of free or liposomal prednisolone phosphate via the tail vein. At 72 h after treatment administration, mice were sacrificed by asphyxiation with CO_2, tumors were harvested and snap frozen in liquid nitrogen. For quantification of prednisolone phosphate in the tumor tissue, 675 μl of phosphate buffered saline (B. Braun, Melsungen, Germany) was added per 250 mg of tumor tissue. Each sample was spiked with 1000 ng of dexamethasone phosphate (Sigma-Aldrich, Germany) as internal standard. Tumor tissue was homogenized in Precellys lysing kit tubes, by 3 sequential 20 second steps of 5000 rpm at 4 °C in a Precellys 24 Dual tissue homogenizer (Bertin Technologies, France). After centrifugation at 10,000 rpm for 5 min at 4 °C, tumor homogenates were collected in glass vials. After liquid-liquid extraction with dichloromethane (Biosolve, The Netherlands) at pH 11, the organic phase was collected and evaporated using a block heater and under nitrogen flow. Prednisolone phosphate levels were quantified by UPLC according to the method described previously [21]. A calibration curve was prepared by spiking tumor tissue with a known concentration of prednisolone and the internal standard dexamethasone phosphate. The limit of detection of this method was ~20 ng/ml.

2.5. miRNA profiling

Frozen tumor tissue stored at −80 °C was transferred into RNAlater-ICE frozen tissue transition solution (Ambion Life Technologies/Thermo Fisher Scientific, Waltham, MA, USA) on dry ice, and subsequently incubated for 24 h at −20 °C according to manufacturer's instructions. Tissues were homogenized using the Precellys 24 Dual Homogenizer and transferred into a polypropylene centrifuge tube. miRNA Homogenate Additive was added and mixed and miRNA fraction was isolated using the miRVANA isolation kit. Isolated small RNAs were sequenced on an Ion Torrent Personal Genome Machine™ Sequencer according to manufacturer's instructions using the Ion Total RNA-Seq kit. Sequences were uploaded to the miRanalyzer software accessible via http://bioinfo2.ugr.es/miRanalyzer/miRanalyzer.php [22] and ranked according to their abundance.

2.6. Stem-loop reverse transcription PCR

Tumor tissue was prepared as described above and RNA isolation was performed using Trizol (Invitrogen) following the manufacturer's protocol. The presence of miR-146b was determined by Stem-Loop RT-PCR as described in Chen et al. [23]. miRNA levels were determined according to standard protocol using home-made primers and SYBRGreen (Bio-Rad, CA, USA). For the stem-loop RT-PCR individual forward primers were designed according to mature miRNA sequence in miRBase 16. As a housekeeping gene U6 was used. RT-PCR was performed on a BioRad CFX96 (CA, USA). Sequences of the primers were.

Stem loop mmu-miR-146b
5′-GTCGTATCCAGTGCAGGGTCCGAGGTATTCGCACTGGATACGAAGC CTAT-3′
Forward mmu-miR-146b
5′ TGCCAGTAGAACUGAATTCCATAGG-3′
RT-PCR Reverse
5′-GTGCAGGGTCCGAGGT-3′
U6 stem loop primer
5′-GTCATCCTTGCGCAGG-3′
U6 forward primer
5′-CGCTTCGGCAGCACATATAC-3′

2.7. Statistical analysis

Statistical analyses were performed using GraphPad Prism software v5.03. A F-test on the overall fit was used to evaluate the differences between individual growth curves. One-way ANOVA in combination with Bonferroni post-testing was used to determine statistical differences in drug accumulation in mammary tumors of free and liposomal treated mice. A value of $p < 0.05$ was considered significant.

3. Results and discussion

3.1. Characterization of liposomes

Liposomes had a size of 0.10 ± 0.06 μm with a polydispersity index <0.1 and a PLP content of 5.1 ± 0.4 mg/ml at a phospholipid concentration of 60 ± 7 μmol lipid/ml (average ± standard deviation of 3 preparations).

3.2. In vitro activity

Corticosteroids have been described to inhibit the proliferation of breast cancer cells [24]. Indeed, when we incubated MDA-MB-486 or MCF-7 mammary carcinoma cells with PLP or LCL-PLP, a concentration-dependent inhibition of cell proliferation was noted, with maximal inhibition approximately 40% for the MDA-MB-486 cells and approximately 50% for the MCF-7 cell line (Fig. 1). The sensitivity

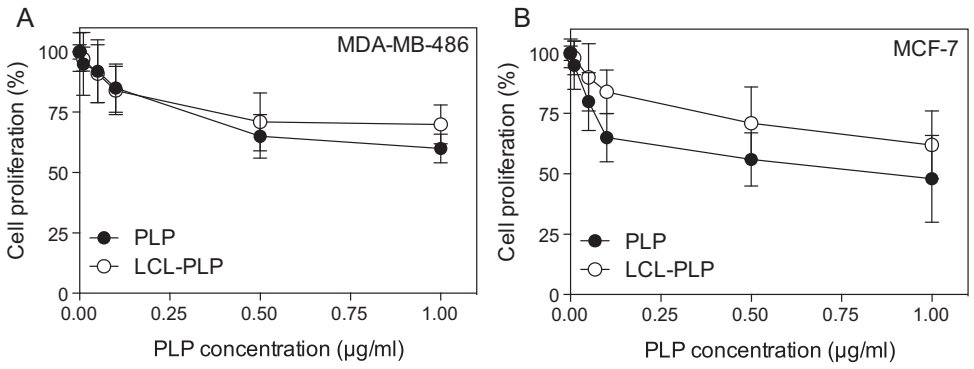

Fig. 1. In vitro effect of free and liposomal PLP on the proliferation of human mammary carcinoma cells. MDA—MB-486 (A) and MCF-7 (B) cell lines were incubated for 48 h with different concentrations of PLP or LCL-PLP, and anti-proliferative effect was determined by ELISA BrdU-colorimetric immunoassay.

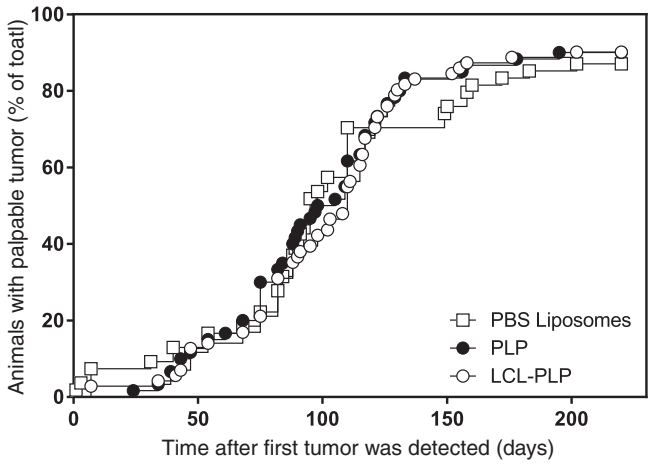

Fig. 2. Time-point of detection of palpable tumors in three experimental groups of MMTV/*neu* mice. Median time for tumor detection was 102 days. No significant differences were noted between experimental groups. Approximately 90% of all animals developed a tumor within 220 days after a tumor was detected at the first mouse.

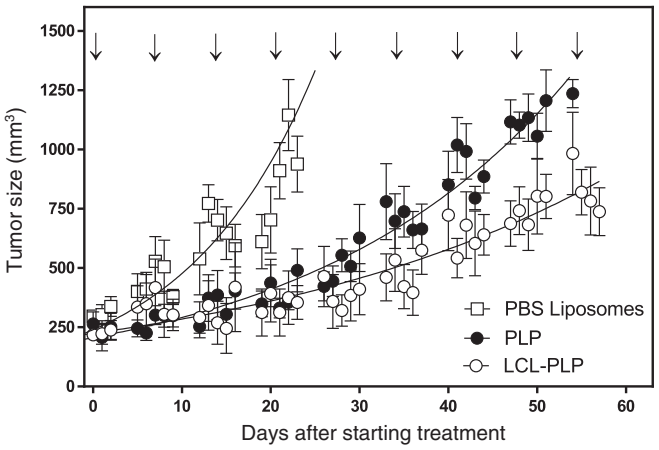

Fig. 3. Effect of PLP and LCL-PLP on tumor growth. Mice received weekly injections of PLP or LCL-PLP (indicated with arrows) at a dose of 20 mg/kg or an equivalent volume of vehicle. Tumor size was measured during the treatment. LCL-PLP inhibits tumor growth significantly more effectively than PLP.

of the breast cancer cells to PLP was approximately 10 times higher than for B16F10 melanoma or C26 colon carcinoma cells [15]. Comparable efficacy was found of PLP and LCL-PLP for MDA-BM-486 cells. The liposomal formulation appeared to be slightly less efficacious than the free drug for MCF-7 cells, which is likely related to the fact that the liposomes need to be taken up and processed for the drug to be released and become active. However, statistical significance was not reached at any of the tested doses when analyzed by non-linear regression.

3.3. MMTV/neu model

Despite the established preclinical value of syngeneic tumor models, such as B16F10 and C26 models, and xenografts, in which tumors are transplanted, the ectopic subcutaneous inoculation of tumor cells in the flank of mice may, by itself, generate an inflammatory response. The exact interference of such "acute" inflammation with tumor development is not known. In addition, this interference may be very different in immune competent mice (for syngeneic tumors) compared to immune-deficient animals (for xenografts). This is especially crucial when developing anti-inflammatory drugs for cancer, as the tissue surrounding the tumor is very important in tumor immunology. In this study, the antitumor effects of liposomal prednisolone phosphate were studied in transgenic mice bearing spontaneous breast carcinomas. The spontaneous development of the tumor in an immune competent host allows us to better assess the potential of targeted anti-inflammatory nanomedicines for tumor therapy.

The spontaneous development of focal mammary adenocarcinomas is well described for transgenic FVB/N c-*neu* mice carrying the unactivated rat HER-2/*neu* proto-oncogene driven by the MMTV promoter. Mice develop tumors after a long latency period (approximately at an age of 4 months) and tumor progression is associated with occurrence of somatic activating mutations in the transgene [19].

Fig. 2 shows the range of time points of appearance of a palpable tumor in the MMTV/*neu* mice. Mice were randomly assigned into three experimental groups. In MMTV/*neu* mice, the time course in which tumors developed was similar for all experimental groups ($p = 0.9$) with a median tumor detection time of 102 days. The curve shows a sigmoidal shape, typical for the Gaussian distribution of the statistical chance of mutation. Approximately 90% of animals developed a tumor within 220 days after the first mouse did. In contrast, our B16F10 melanoma model previously showed a much faster tumor development. In this model, 2 days after the first tumor was detected, the majority of animals had a palpable tumor. Over 95% of animals developed a tumor within 1 week after the first tumor was detected [12].

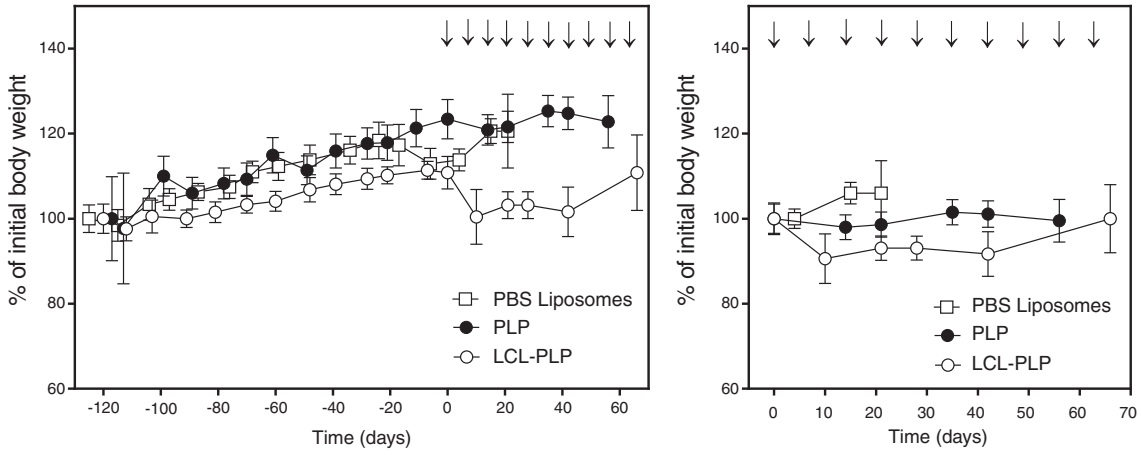

Fig. 4. Effect of PLP and LCL-PLP on body weight. Mice received weekly injections of PLP or LCL-PLP (indicated with arrows) at a dose of 20 mg/kg or an equivalent volume of vehicle. LCL-PLP induces a drop in bodyweight of approximately 10% after initiation of treatment. (A) Percentage of initial body weight throughout the study; (B) Percentage of initial body weight after starting the treatment i.e. day 0.

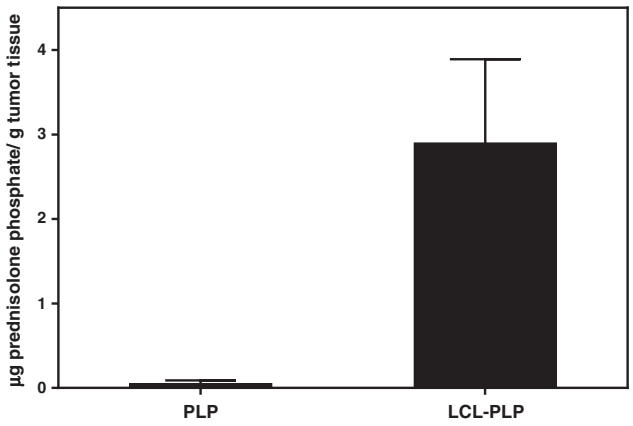

Fig. 5. Prednisolone phosphate levels in MMTV/*neu* tumors at 72 h after administration of 20 mg/kg of PLP (liposomal and/or free). Transgenic FVB/N c-*neu* transgenic mice (MMTV/*neu*), $n = 4$, received a single intravenous administration of 20 mg prednisolone phosphate/kg free (PLP) or in the liposomal form (LCL-PLP) when tumors reached a volume of approximately 200 mm^3. Mice were sacrificed 72 h after drug injection and tumors harvested and snap frozen. Prednisolone phosphate was extracted and quantified by UPLC. In free PLP group, prednisolone phosphate level was below limit of detection. Data presented as mean ± SEM.

3.4. In vivo efficacy

The three treatment groups were assigned to receive vehicle (i.e. PBS) liposomes or 20 mg/kg prednisolone phosphate in free or liposomal form. Mice were treated when tumors reached a volume of 200 mm^3. Treatments were administered once weekly until the tumor volume reached the humane endpoint (>1500 mm^3). In the B16F10 model, only LCL-PLP treatment inhibited tumor proliferation and the free drug was not effective. Tumor doubling time for vehicle controls was 2.2 days for vehicle controls (95% CI 2.0–2.5), 3.2 days for PLP (95% CI 2.3–4.5), and 4.2 days for LCL-PLP (95% CI 3.1–7.4) ($p < 0.05$ LCL-PLP compared to control) in this model [15].

In the MMTV/*neu* model, tumor volumes were significantly smaller after liposomal prednisolone treatment as compared to free drug or vehicle (Fig. 3). Average tumor growth curves were plotted until one or more mice reached the humane endpoint in that group. Tumor doubling time was 10.5 days for vehicle controls (95% CI 8.5–13.6), 20.7 days for PLP (95% CI 18.0–22.8), and 35.5 days for LCL-PLP (95% CI 28.7–46.4) ($p < 0.05$; PLP and LCL-PLP compared to control, and LCL-PLP compared to PLP). Overall, these results show that the tumor-inhibitory activity of LCL-PLP is maintained in a spontaneous mammary carcinoma model. Although tumor growth is smaller than in the implantation models that we previously studied it is still substantially faster than in the human disease.

When examining body weight of the mice, we observed a steady increase in body weight until the moment when treatment was initiated. At that time-point we observed an approximately 10% loss in body weight only for the LCL-PLP treated animals in the MMTV/*neu* model (Fig. 4). This is similar to the body weight loss observed after LCL-PLP treatment in B16F10 tumor-bearing animals.

3.5. Tumor accumulation of LCL-PLP

To investigate if long circulating liposomes accumulate in the tumor tissue of MMTV/*neu* mice, prednisolone levels were quantified in the tumor tissue 72 h after administration of 20 mg prednisolone/kg. As shown in Fig. 5, free drug could not be detected in the tumor tissue at 72 h after drug administration, similar to B16F10 tumor tissue. In contrast, liposomal drug could still be recovered. The passive tumor accumulation of the liposomal drug is known to rely on the EPR effect, which is a phenomenon that is not applicable to all tumors and intratumoral areas to the same extent. Because of the rapid growth of subcutaneously implanted tumors, we hypothesized that blood vessels have less time to develop properly and we expected the EPR effect to be more prominent in implanted tumors than slow-growing spontaneous tumors. Our results suggest that despite the developmental, structural and morphological differences between these two tumor models, liposomes extravasate from the circulation in a spontaneous tumor model to the same extent as syngeneic tumor models, which to our knowledge has never been demonstrated before. These results imply that the capillary permeability is increased by angiogenesis and inflammatory reactions to an equal extent in the MMTV/*Neu* model as in the B16F10 and C26 models.

3.6. Micro RNA analysis

To characterize the molecular response within the tumor due to liposomal PLP treatment we analyzed miRNA profiles of dissected tumor tissues. In total >200 miRNA species were identified. The ten most abundant miRNAs constituted 53% of the total number of miRNA sequences that were detected. Nine of the top ten miRNA species were the same between treatments (Table 1). These nine miRNA species of the let-7 family and miR-16, -21, -23b, -24, -27b, -30a, and -30c are known to be involved in cancer, and their expression is both related to tumor promoting and inhibiting activities. One miRNA, miR-146b appeared to be strongly upregulated by liposomal PLP treatment. Very few copies were detected in the controls but this miRNA rose to the top 10 after liposomal PLP treatment.

Interestingly, expression of miR-146a/b has been found to be downregulated in breast cancer [25]. MiR-146b expression is reported to be associated with an inhibition of inflammation through downregulation of NF-κB activity and subsequent decrease in IL-6 production [26]. IL-6 induces expression of miR-146b by activating STAT3, which negatively

Table 1
Top ten miRNA profiles of control and LCL-PLP-treated mice.

Rank control	miRNA	Rank LCL-PLP	Role
1	mmu-miR-27b	6	Pro-oncogenic factors miR-23b and miR-27b are regulated by Her2/Neu, EGF, and TNF-α in breast cancer.
2	mmu-miR-23b	3	
3	mmu-miR-30a	7	MicroRNA-30a suppresses breast tumor growth and metastasis by targeting metadherin.
4	mmu-miR-24	1	MicroRNA miR-24 enhances tumor invasion and metastasis by targeting PTPN9 and PTPRF to promote EGF signaling.
5	mmu-let-7c	5	LIN28: a regulator of tumor-suppressing activity of let-7 microRNA in human breast cancer.
6	mmu-miR-30c	2	Deregulated miRNAs in hereditary breast cancer revealed a role for miR-30c in regulating KRAS oncogene.
7	mmu-miR-26a	8	Trastuzumab produces therapeutic actions by upregulating miR-26a and miR-30b in breast cancer cells.
8	mmu-let-7f	10	LIN28: a regulator of tumor-suppressing activity of let-7 microRNA in human breast cancer.
9	mmu-miR-21	4	MicroRNA-21 as an indicator of aggressive phenotype in breast cancer.
10	mmu-miR-16	12	Downregulation of the tumor-suppressor miR-16 via progestin-mediated oncogenic signaling contributes to breast cancer development.
32	mmu-miR-146b	9	Breast cancer metastasis suppressor 1 up-regulates miR-146, which suppresses breast cancer metastasis. MicroRNA-146 represses endothelial activation by inhibiting pro-inflammatory pathways. MicroRNAs in resolution of acute inflammation: identification of novel resolvin D1-miRNA circuits.

controls the activity of NF-κB [27]. However, in cancer cells, STAT3-induced expression of miR-146b is reduced leading to a disruption in the negative feedback loop and transforming cells to malignant phenotype [28]. Furthermore, the FOXP3-miR-146-NF-κB axis was recently identified as a therapeutic target in breast cancer due to its involvement in proliferation and survival of breast cancer cells [29,30]. FOXP3 induction in breast epithelial cells results in upregulation of miR-146a/b. Earlier studies showed that glucocorticoids upregulate expression of FOXP3 in Treg cells [31]. Secondly, miR-146a/b downregulates expression of the *BRCA1* gene by directly binding to its 3'UTR [32]. This correlates with the potent anti-inflammatory profile of liposomal PLP. Indeed, these results are in line with a study by Phuong et al. showing that overexpression of miR-146 inhibits proliferation of breast cancer cells [33]. Therefore, miR-146b was analyzed in more detail with quantitative RT-PCR. These results confirmed the observed increased abundancy of miR-146b. An 18-fold increased expression was measured compared to control animals (Fig. 6). For PLP a non-significant 4.5 fold increase was noted.

The spontaneous tumor models resemble the human disease better than xenograft models. Still, there are several factors in human breast cancers that are not fully replicated in these spontaneous models. For example, it is known that the glucocorticoid receptor changes its cellular location during breast cancer development and in general there is a pattern towards the decline in glucocorticoid-receptor expression from normal via precancerous lesions to invasive breast carcinoma [34]. Additionally, the activation of the glucocorticoid receptor induces expression and activity of an enzyme involved in the deactivation of estrogen and may in this way interfere with the growth of hormone-dependent tumors [35]. However, the majority of spontaneous breast cancer models are estrogen receptor negative and hormone independent [36]. Immunohistochemistry studies in mammary tissue from MMTV/unactivated *neu* transgenic mice have shown that it is composed of different subpopulations of proliferating cells present in hyperplastic mammary ducts with respect to estrogen-α and *neu* expression [37]. These differences may impact the translatability of findings in the spontaneous models to the human disease.

Taken together, liposomal glucocorticoids also inhibit tumor growth in the spontaneous MMTV/*neu* model, similar to syngeneic B16F10 and C26 models. Although tumor growth kinetics are remarkably different between the two models, this apparently does not translate in different enhanced permeability and retention-mediated liposome accumulation kinetics. To our knowledge, this is the first time that tumor accumulation of a drug delivered by a liposomal delivery system is studied and quantified in a spontaneous tumor model. A study of the miRNA profile in the tumor tissue with and without treatment revealed that the top ten most abundant miRNA were remarkably similar. Many of the prominent miRNAs that are associated with human breast cancer were also highly expressed in the murine model. One notable exception was miR-146b. This miRNA was strongly upregulated after treatment. The increased expression of miR-146b in liposomal PLP treated tumors suggests that liposomal PLP can inhibit tumor growth at least in part by modulating the FOXP3-miR-146-NF-κB axis.

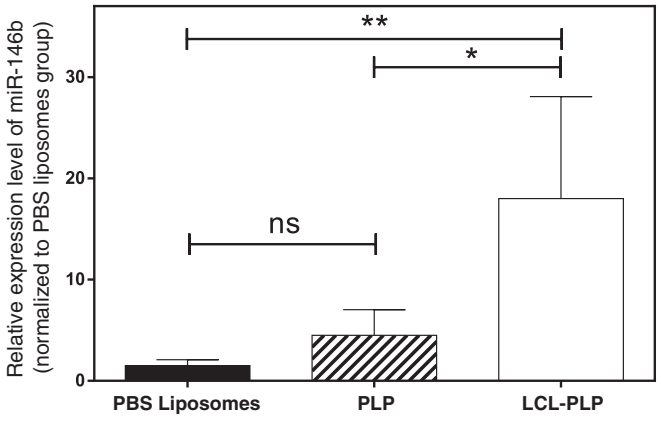

Fig. 6. MiR-146b abundancy in PLP and LCL-PLP-treated tumors. Transgenic FVB/N c-*neu* transgenic mice (MMTV/*neu*), $n = 4$, received a single intravenous administration of 20 mg prednisolone/kg free (PLP) or in the liposomal form (LCL-PLP) when tumors reached approximately 200 mm^3. Mice were sacrificed 72 h after drug injection and miRNA levels were detected in tumors. MiR-146b showed an 18-fold increased expression in LCL-PLP-treated mice when compared to vehicle control animals ($p < 0.01$), whereas PLP-treated mice only showed a non-significant 4.5-fold change.

Liposomal glucocorticoids act by modulating the pro-inflammatory tumor micro-environment that has a net positive effect on tumor growth. But this therapeutic approach is not curative by itself it is only inhibiting tumor growth. A logical next step would be to combine treatment with cytotoxic chemotherapeutic agents, as conventional agents or in nanocarrier-encapsulated form, to explore synergy between these two therapeutic modes of action. Since the stromal cells in the tumor can modulate chemotherapeutic resistance of tumor cells, such a two-pronged may improve therapeutic outcome compared to either treatment alone.

Acknowledgements

The research of MC and RMS is supported by grant UFA 07947 of the Technology Foundation STW/Netherlands Organization for Scientific Research NWO- Innovational Research Incentives Scheme VIDI. The authors would like to thank Ebel Pieters and Willemiek Kassing-van der Ven (Utrecht University) for their assistance with the animal work.

References

[1] D. Hanahan, L.M. Coussens, Accessories to the crime: functions of cells recruited to the tumor microenvironment, Cancer Cell 21 (2012) 309–322.
[2] B. Ruffell, A. Au, H.S. Rugo, L.J. Esserman, E.S. Hwang, L.M. Coussens, Leukocyte composition of human breast cancer, Proc. Natl. Acad. Sci. U. S. A. 109 (2012) 2796–2801.
[3] D. Hanahan, R.A. Weinberg, Hallmarks of cancer: the next generation, Cell 144 (2011) 646–674.
[4] E. Elinav, R. Nowarski, C.A. Thaiss, B. Hu, C. Jin, R.A. Flavell, Inflammation-induced cancer: crosstalk between tumours, immune cells and microorganisms, Nat. Rev. Cancer 13 (2013) 759–771.
[5] R.M. Schiffelers, G. Storm, Liposomal nanomedicines as anticancer therapeutics: beyond targeting tumor cells, Int. J. Pharm. 364 (2008) 258–264.
[6] L.M. Coussens, L. Zitvogel, A.K. Palucka, Neutralizing tumor-promoting chronic inflammation: a magic bullet? Science 339 (2013) 286–291.
[7] M. Coimbra, S.A. Kuijpers, S.P. van Seters, G. Storm, R.M. Schiffelers, Targeted delivery of anti-inflammatory agents to tumors, Curr. Pharm. Des. 15 (2009) 1825–1843.
[8] M. Banciu, R.M. Schiffelers, J.M. Metselaar, G. Storm, Utility of targeted glucocorticoids in cancer therapy, J. Liposome Res. 18 (2008) 47–57.
[9] J. Folkman, R. Langer, R.J. Linhardt, C. Haudenschild, S. Taylor, Angiogenesis inhibition and tumor regression caused by heparin or a heparin fragment in the presence of cortisone, Science 221 (1983) 719–725.
[10] M. Coimbra, C.J. Rijcken, M. Stigter, W.E. Hennink, G. Storm, R.M. Schiffelers, Antitumor efficacy of dexamethasone-loaded core-crosslinked polymeric micelles, J. Control. Release 163 (2012) 361–367.
[11] Y. Mao, G. Triantafillou, E. Hertlein, W. Towns, M. Stefanovski, X. Mo, D. Jarjoura, M. Phelps, G. Marcucci, L.J. Lee, D.M. Goldenberg, R.J. Lee, J.C. Byrd, N. Muthusamy, Milatuzumab-conjugated liposomes as targeted dexamethasone carriers for therapeutic delivery in CD74+ B-cell malignancies, Clin. Cancer Res. 19 (2013) 347–356.
[12] M. Banciu, J.M. Metselaar, R.M. Schiffelers, G. Storm, Liposomal glucocorticoids as tumor-targeted anti-angiogenic nanomedicine in B16 melanoma-bearing mice, J. Steroid Biochem. Mol. Biol. 111 (2008) 101–110.
[13] M.E. Lobatto, Z.A. Fayad, S. Silvera, E. Vucic, C. Calcagno, V. Mani, S.D. Dickson, K. Nicolay, M. Banciu, R.M. Schiffelers, J.M. Metselaar, L. van Bloois, H.S. Wu, J.T. Fallon, J.H. Rudd, V. Fuster, E.A. Fisher, G. Storm, W.J. Mulder, Multimodal clinical imaging to longitudinally assess a nanomedical anti-inflammatory treatment in experimental atherosclerosis, Mol. Pharm. 7 (2010) 2020–2029.
[14] E. Kluza, S.Y. Yeo, S. Schmid, D.W. van der Schaft, R.W. Boekhoven, R.M. Schiffelers, G. Storm, G.J. Strijkers, K. Nicolay, Anti-tumor activity of liposomal glucocorticoids: the relevance of liposome-mediated drug delivery, intratumoral localization and systemic activity, J. Control. Release 151 (2011) 10–17.
[15] R.M. Schiffelers, J.M. Metselaar, M.H. Fens, A.P. Janssen, G. Molema, G. Storm, Liposome-encapsulated prednisolone phosphate inhibits growth of established tumors in mice, Neoplasia 7 (2005) 118–127.
[16] A.D. Borowsky, Choosing a mouse model: experimental biology in context–the utility and limitations of mouse models of breast cancer, Cold Spring Harb. Perspect. Biol. 3 (2011) a009670.

[17] K. Hansen, C. Khanna, Spontaneous and genetically engineered animal models; use in preclinical cancer drug development, Eur. J. Cancer 40 (2004) 858–880.
[18] S.E. Gould, M.R. Junttila, F.J. de Sauvage, Translational value of mouse models in oncology drug development, Nat. Med. 21 (2015) 431–439.
[19] C.T. Guy, M.A. Webster, M. Schaller, T.J. Parsons, R.D. Cardiff, W.J. Muller, Expression of the neu protooncogene in the mammary epithelium of transgenic mice induces metastatic disease, Proc. Natl. Acad. Sci. U. S. A. 89 (1992) 10578–10582.
[20] G. Rouser, S. Fkeischer, A. Yamamoto, Two dimensional then layer chromatographic separation of polar lipids and determination of phospholipids by phosphorus analysis of spots, Lipids 5 (1970) 494–496.
[21] J.M. Metselaar, M.H. Wauben, J.P. Wagenaar-Hilbers, O.C. Boerman, G. Storm, Complete remission of experimental arthritis by joint targeting of glucocorticoids with long-circulating liposomes, Arthritis Rheum. 48 (2003) 2059–2066.
[22] M. Hackenberg, N. Rodriguez-Ezpeleta, A.M. Aransay, miRanalyzer: an update on the detection and analysis of microRNAs in high-throughput sequencing experiments, Nucleic Acids Res. 39 (2011) W132–W138.
[23] C. Chen, D.A. Ridzon, A.J. Broomer, Z. Zhou, D.H. Lee, J.T. Nguyen, M. Barbisin, N.L. Xu, V.R. Mahuvakar, M.R. Andersen, K.Q. Lao, K.J. Livak, K.J. Guegler, Real-time quantification of microRNAs by stem-loop RT-PCR, Nucleic Acids Res. 33 (2005), e179.
[24] S. Hundertmark, H. Buhler, M. Rudolf, H.K. Weitzel, V. Ragosch, Inhibition of 11 beta-hydroxysteroid dehydrogenase activity enhances the antiproliferative effect of glucocorticosteroids on MCF-7 and ZR-75-1 breast cancer cells, J. Endocrinol. 155 (1997) 171–180.
[25] Y. Li, Y. Xu, C. Yu, W. Zuo, Associations of miR-146a and miR-146b expression and breast cancer in very young women, Cancer Biomark. 15 (2015) 881–887.
[26] D. Bhaumik, G.K. Scott, S. Schokrpur, C.K. Patil, J. Campisi, C.C. Benz, Expression of microRNA-146 suppresses NF-kappaB activity with reduction of metastatic potential in breast cancer cells, Oncogene 27 (2008) 5643–5647.
[27] M. Xiang, N.J. Birkbak, V. Vafaizadeh, S.R. Walker, J.E. Yeh, S. Liu, Y. Kroll, M. Boldin, K. Taganov, B. Groner, A.L. Richardson, D.A. Frank, STAT3 induction of miR-146b forms a feedback loop to inhibit the NF-kappaB to IL-6 signaling axis and STAT3-driven cancer phenotypes, Sci. Signal. 7 (2014) ra11.
[28] S.R. Walker, M. Xiang, D.A. Frank, STAT3 activity and function in cancer: modulation by STAT5 and miR-146b, Cancers (Basel) 6 (2014) 958–968.
[29] R. Liu, C. Liu, D. Chen, W.H. Yang, X. Liu, C.G. Liu, C.M. Dugas, F. Tang, P. Zheng, Y. Liu, L. Wang, FOXP3 controls an miR-146/NF-kappaB negative feedback loop that inhibits apoptosis in breast cancer cells, Cancer Res. 75 (2015) 1703–1713.
[30] D.M. Etikala, R. Liu, L. Wang, FOXP3-microRNA-146-NF-kappaB as oncotarget, Oncoscience 2 (2015) 839–840.
[31] C. Prado, J. Gomez, P. Lopez, B. de Paz, C. Gutierrez, A. Suarez, Dexamethasone upregulates FOXP3 expression without increasing regulatory activity, Immunobiology 216 (2011) 386–392.
[32] A.I. Garcia, M. Buisson, P. Bertrand, R. Rimokh, E. Rouleau, B.S. Lopez, R. Lidereau, I. Mikaelian, S. Mazoyer, Down-regulation of BRCA1 expression by miR-146a and miR-146b-5p in triple negative sporadic breast cancers, EMBO Mol. Med. 3 (2011) 279–290.
[33] N.T. Phuong, S.K. Kim, J.H. Im, J.W. Yang, M.C. Choi, S.C. Lim, K.Y. Lee, Y.M. Kim, J.H. Yoon, K.W. Kang, Induction of methionine adenosyltransferase 2A in tamoxifen-resistant breast cancer cells, Oncotarget 7 (2016) 13902–13916.
[34] M. Vilasco, L. Communal, N. Mourra, A. Courtin, P. Forgez, A. Gompel, Glucocorticoid receptor and breast cancer, Breast Cancer Res. Treat. 130 (2011) 1–10.
[35] H. Gong, M.J. Jarzynka, T.J. Cole, J.H. Lee, T. Wada, B. Zhang, J. Gao, W.C. Song, D.B. DeFranco, S.Y. Cheng, W. Xie, Glucocorticoids antagonize estrogens by glucocorticoid receptor-mediated activation of estrogen sulfotransferase, Cancer Res. 68 (2008) 7386–7393.
[36] P. Taneja, D.P. Frazier, R.D. Kendig, D. Maglic, T. Sugiyama, F. Kai, N.K. Taneja, K. Inoue, MMTV mouse models and the diagnostic values of MMTV-like sequences in human breast cancer, Expert. Rev. Mol. Diagn. 9 (2009) 423–440.
[37] G. Shyamala, Y.C. Chou, R.D. Cardiff, E. Vargis, Effect of c-neu/ErbB2 expression levels on estrogen receptor alpha-dependent proliferation in mammary epithelial cells: implications for breast cancer biology, Cancer Res. 66 (2006) 10391–10398.